

# Ant colony optimization-induced route optimization for enhancing driving range of electric vehicles

Gunasekaran Manogaran<sup>1</sup> | P. Mohamed Shakeel<sup>2</sup> | Vishnu Priyan R<sup>3</sup> | Naveen Chilamkurti<sup>4</sup> | Abhishekh Srivastava<sup>1</sup>

<sup>1</sup>Big Data Scientist, University of California Davis, Davis, California

<sup>2</sup>Faculty of Information and Communication Technology, Universiti Teknikal Malaysia Melaka, Durian Tunggal, Melaka, Malaysia

<sup>3</sup>Department of Computer Science, Christ College of Engineering and Technology, Pondicherry University, Puducherry, India

<sup>4</sup>Department of Computer Science and IT, La Trobe University, Melbourne, Victoria, Australia

## Correspondence

Gunasekaran Manogaran, Big Data Scientist Gunasekaran Manogaran, University of California Davis, Davis, CA, USA.

Email: gmanogaran@ucdavis.edu

## Summary

Electric vehicles (EVs) are the emerging solution for pollution-free transportation systems in the modern era. Battery-operated motor-powered electric vehicles serve the purpose of transportation with in-time recharging ability. Routing and traversing locations using EVs demand optimal route selection for retaining delay and power of the vehicle. This manuscript proposes a fitness-ant colony optimization (FACO)-based route optimization for improving the driving range of EVs. FACO works in two phases: conditional route discovery and range-sustained traversing to control delay and to deprive EV failures because of earlier power drain. In range-sustained phase, the fitness of the traversing route is framed by considering the inputs of power and travel time of the EV for ensuring construction of optimal touring paths. The EVs are directed to traverse the paths defined through ACO, after which the available paths are further attuned to identify the most efficient route depending on the braking and battery power of the vehicle. This optimization balances both power and its variants along with travel time for improving the driving range of the EV before it actually drains out. The optimization technique is assessed using arbitrary road and delivery point simulation with real-time configurations to demonstrate the effectiveness of the proposed method. Experimental results demonstrate the consistency of the proposed FACO by increasing driving distance and delivery point visits. This optimization also achieves lesser power depletion retaining higher charging level with lesser waiting time.

## KEYWORDS

ant colony optimization, electric vehicle, fitness path construction, route selection, vehicle battery charging

## 1 | INTRODUCTION

Intelligent transportation system (ITS) is one of the promising technologies forming a structural block of smart-city architectures. ITS is designed to handle transportation demands sustaining environmental protection. With the support of backhauling networks and communication links, these systems provide uninterrupted services and safer transportation for the increasing vehicle density.<sup>1,2</sup> In a smart-city environment, ITS is planned to provide solutions for traffic congestions, pollution, communications, entertainment, service discovery, etc. The indispensable function of ITS is to

initiate routing services that provides the foresaid solutions. Routing services rely on the infrastructure and other vehicular units to ensure seamlessness in connectivity and service retrieval. Routing services are used to identify optimal neighbors and routes to gather location, energy, and emission information.<sup>3,4</sup>

Emerging smart city with ITS focuses on three goals: efficient transportation functions, emission zero or pollution free, and renewable energy vehicles. In order to facilitate renewable energy sources and to control emissions, electric vehicles (EVs) are manufactured as an alternate for gasoline/petroleum vehicles.<sup>5-8</sup> Onboard battery sources equipped in the EVs are considered as environmental and energy saving solutions in smart-city environment.<sup>9</sup> The most prominent requirement for the EVs is its battery recharging process that is influenced by the availability and swiftness of the charging infrastructure.<sup>10</sup> Evolution of EVs in the eco-friendly smart-city environment faces a variety of challenges: energy constraint nature, driving range, and deployment of charging stations (CSs).<sup>11,12</sup> With the available grid-to-vehicle charging infrastructure, EV is fast charged to avoid power interruptions and vehicle halts amid a service.

EVs pursue the shortest or energy-efficient paths to prevent earlier battery drain. Routing in this vehicular network needs to achieve lesser travel time and identifying efficient charging infrastructures. Therefore, conventional routing algorithms with distance metric do not suit for EVs. Routing solutions for EVs are intended to solve path planning problems, negative edge connectivity issues, and cost-effective recharging.<sup>5,13</sup> Constructing charging infrastructures within a limited region increases cost of deployment and is not advisable for a conservative smart-city environment. Planned steady-state battery operations sustain the lifetime of the EV before running out of communication.<sup>14</sup>

## 2 | RELATED WORKS

Hongming Yang et al.<sup>15</sup> proposed a crowd-sensing-based navigation strategy for EVs. The route selection model designed minimizes the travel and charging cost of the users. This model requires complex evaluation with the increase in neighbor density for identifying the near-optimal routes.

Optimal route discovery with the traffic awareness is facilitated by real-time intersection-based segments aware routing<sup>16</sup> in vehicular ad hoc networks (VANETs). This method minimizes communication overhead by predicting segment failures in advance; contrarily, the round-trip time observed is high.

iCAR-II<sup>17</sup> is introduced to minimize delay in multihop vehicular applications aided by internet services. With the help of network connectivity information and location update, iCAR constructs a global topology to improving routing performance. The number of infrastructure communications for improving routing optimality is considerably high.

Moving zone-based routing protocol is proposed by Dan Lin et al.<sup>18</sup> that assimilates indexing and object modeling techniques for efficient resource utilization. Vehicular mobility, storage, and network management are assisted with this routing protocol for improving transmission efficiency.

Ad hoc network-based routing protocol is introduced for conserving the battery of EVs in Song et al.<sup>19</sup> Without the support of external resources/backhaul networks, the protocol is effective in retrieving the battery status of the EVs. The complexity of a direct ad hoc protocol is its periodic beacon update for ensuring neighbor connectivity.

To meet with the supply demands in smart cities, autonomous vehicles logistic system (AVLS)<sup>20</sup> is introduced. Joint routing and charging problems are addressed to aid flexibility and of autonomous vehicles in smart cities.

Model predictive control<sup>21</sup> is a multiobjective optimization for reducing complexity in route discovery. The route discovery is concentrated for facilitating wireless and charging solutions for EVs. The optimality of the solution swings between distance and cost independently, other than joint optimization.

Tao Chen et al.<sup>22</sup> considered the charging cost and energy effectiveness of charging an EV for discovering optimal routes. The authors have proposed a mathematical model with nonenvironmental considerations.

Graph-based shortest path algorithm<sup>23</sup> is designed to improve the driving range of the vehicles by efficient use of mobile energy disseminators. The displacement of the vehicle for the availability of energy disseminators increases the waiting time of the vehicles.

With the idea of data mining, a novel routing algorithm for improving efficiency in EVs is proposed in Bozorgi et al.<sup>13</sup> The efficiency is achieved by improving the driving range and battery life span. Querying volumes of vehicle-related information requires complex storage and processing.

Schuster OVE et al.<sup>24</sup> proposed a brokerage-based routing solution for charge-demanding EVs. Besides, a charge-station-concentrated load balancing and low voltage problems are also addressed.

A scheduling scheme for minimizing request servicing time of EVs is proposed in Boysen et al.<sup>25</sup> This scheduling organizes vehicle contact ensuring planned location and timely charging.

Multimetric geographic routing<sup>26</sup> accounts the environmental conditions for selecting next hop vehicular neighbors. This method ensures connection endurance in vehicular ad hoc networks.

Michael Schneider et al<sup>27</sup> proposed an adaptive variable neighborhood search to address intermediate halt point's problem in vehicular routing. Local search requires recursive updates, increasing the communication complexity.

Genetic algorithm-based route optimization for minimizing delay in charging and traveling of EV is introduced in Shao et al.<sup>5</sup> With the combination of genetic and Dijkstra algorithms, the travel time and distance are planned for the EV to conserve its battery power and improve driving range.

From the above survey, it is clear that route and driving range optimization of the EVs improves communication productivity. Multiobjective optimization is trapped in local optima as the different solutions provided by the factors are not in unison. Considering this predominance, this manuscript is addressing the routing and power depletion issues in EVs through a fitness-based evaluation. Fitness evaluation supported by conditional routing prevents local optima through mutual exclusion travel plan of the EVs. Therefore, the contributions of the manuscript are summarized as follows:

- Design of a condition-based route discovery that confines additional delay by formulating adaptable routing plan for the EVs. This routing is built over ant colony optimization, and it accounts the intersection of the delivery points (DPs) to minimize waiting delay and mutual visit sharing.
- Fitness-dependent range-sustained routing to improve the driving range of the vehicle with controlled power exploitation. Fitness frames rules based on power and delay factors conjointly to outwit local optima, resulting in power conservation and improved driving range of EVs.
- Extensive analysis of the proposed method is done through self and comparative analysis with respect to travel distance, CSs, and vehicle density. This part proves the consistency of the proposed method with the detailed summary of analysis.

### 3 | FITNESS-BASED ANT COLONY OPTIMIZATION FOR ENHANCING ROUTE DISCOVERY OF EVS

#### 3.1 | Scenario

Figure 1 illustrates the EV scenario and its route plan.

The components illustrated in an EV scenario are described as follows:

**Charging station (CS)** CS serves the purpose of recharging the draining/drained vehicle battery amidst its operation time. CS require special infrastructure making it expensive. Therefore, the CS are deployed sparsely.

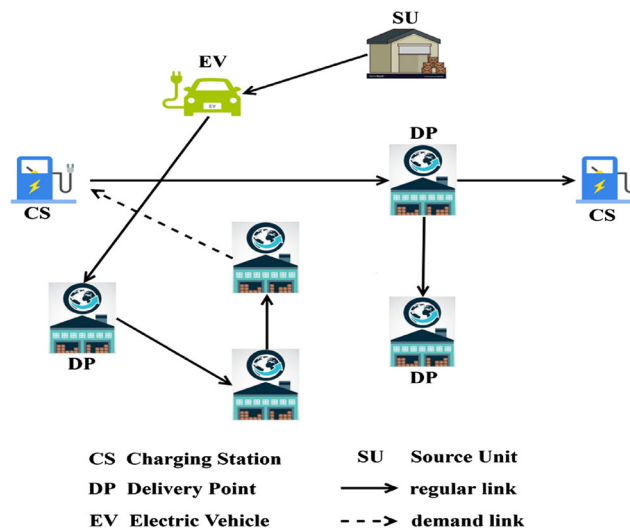


**FIGURE 1** Typical electric vehicle (EV) scenario

Delivery point (DP)	The DP is similar to a collection hub, where the requested service is aggregation. The service is delivered using electric vehicles (EVs). On receiving the service, DP acknowledges the EV. The density of DP varies with the population of a city.
Electric vehicle (EV)	The EV is an autonomous battery-operated vehicle used for various purposes. The EV possesses random mobility and is free to move in any direction. As the vehicle is battery powered, its speed is limited, whereas it does not pollute the environment.
Source unit (SU)	EVs instigate their route from a fixed place called source units (SUs). SU serves as the data providing center for all the DPs.

The route between two DPs or SU to DP is a regular link (rl); if the EV requires recharging, then demand links (dl) are established.

### 3.2 | Assumptions

- The list of DPs to be visited is initially fed to the EV.
- EVs recharge their battery at the end of each list completion, irrespective of the number of recharge amidst the visiting process.

### 3.3 | Problem definition

Consider an open area with “v” EVs, connected to DPs using regulator links (rl) and CS using demand link (dl). The connectivity is modeled as a graph  $G = (n, rl) \forall t$  or  $G = (n, dl) \forall t_c$ , where  $t$  is the time observed for an EV any operation and  $t_c$  is the charging time of EV and  $t_c \leq t$ . In a distance-directed routing optimization, the visiting places of the EV are reached in time. The delay in visiting a neighbor/a DP is ensured to be less through proper route discovery; conventional optimization methods identify shortest distance neighbors/routes to reach the delivery units. Looped routes and linear routing solutions increase the traveling time of the vehicles such that  $t_c > t$ . This will leave the vehicle battery in a drain state, and the travel range of the vehicle is not achieved.

### 3.4 | Proposed methodology

The proposed fitness-ant colony optimization (FACO) for EV route optimization is segregated into two phases: conditional route discovery and range-sustained traversing.

Conditional route discovery identifies possible visiting paths to the DPs in a progressive manner. Fitness function optimizes visiting plan to retain  $t_c < t$ . This aim of the fitness function is to maintain the charging time lesser than the operation time of the vehicle. If this is not achieved, the vehicle drains out of energy, and the traversing is unprofitable. Both the phases work in a cooperative manner to minimize delay and conserve vehicle energy so as to achieve higher driving range. Range-sustained traversing relies on the solutions of conditional route discovery that identifies delay-less routes for vehicle movement. Figure 2 illustrates the process of the proposed FACO.

### 3.5 | Conditional route discovery

In a conventional ACO process, the ant agents visit the destination in different paths. They visit different neighbors to reach the destination; the number of neighbors determines the ant agents. Different from the conventional process of ACO, fixed number of ants is used to discover the routes to the destination. The destination here refers to the longest DP; routes to the DPs are discovered in the order of their location. The objective to be achieved in this route discovery is lesser delay. Therefore, the pheromone of ants is defined to meet the condition of achieving lesser delay. Let an EV travel from one DP  $i$  to  $j$ ; then, the time of travel ( $t_{tr}$ ) is estimated using Equation (1) as

$$t_{tr} = \frac{\text{dist}_{tr}^t}{\text{ev}_v^t}, \quad (1)$$

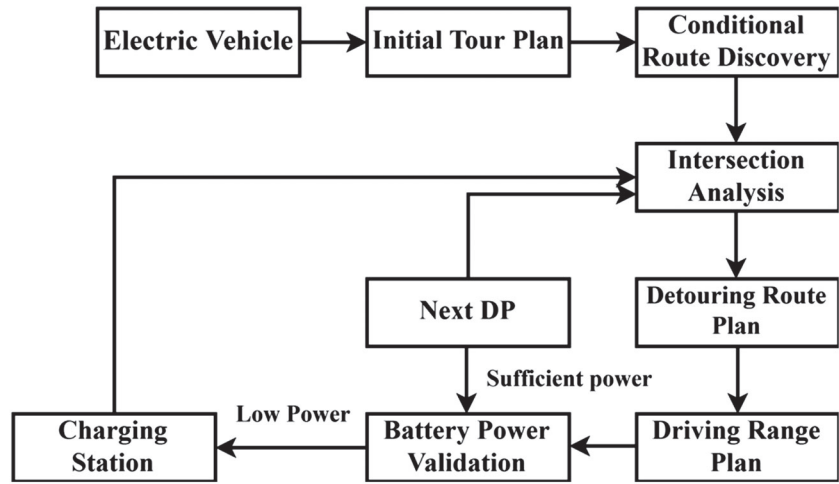


**FIGURE 2** Process of fitness-ant colony optimization (FACO)

where  $\text{dist}_r^t$  and  $\text{ev}_v^t$  are the distance and velocity of the EV in the route  $r$  at time  $t$ . The total time taken for an EV for visiting all the links (both regular and demand) is estimated as  $\Delta t_{tr} = \sum_{v \in r} \sum_{i=1}^n \frac{\text{dist}_r^i}{\text{ev}_v^i}$ , where  $n$  is the time period for the EV to visit all the routes. Let  $\mathcal{O}(t)$  be the objective function for which  $\min\{\Delta t_{tr}\} \forall r$  or  $\min\{t_{tr}\}$  is to be achieved. Initially, the ant agents are generated at the SU and are made to traverse available routes to each of the DP. The probability that an ant visits DP  $j$  after leaving DP  $i$  is estimated as

$$\rho_{ij}^{\text{dist}}(t) = \frac{[\tau_{ij}(t)]^\alpha \cdot [\eta_{ij}]^\beta}{\sum_{j \in r} [\tau_{ij}(t)]^\alpha \cdot [\eta_{ij}]^\beta}, \quad (2)$$

where  $\tau_{ij}$  is the pheromone absorption rate in the route  $(i,j)$  and  $\eta_{ij}$  is the heuristic value for  $t_{tr}$ .  $\alpha$  and  $\beta$  are the balancing constant and  $\alpha + \beta = 1$ . The rate of pheromone absorption declines with varying time interval in a route  $(i,j)$  that is estimated as

$$\tau_{ij} = (1 - \omega) * \tau_{ij} + \sum_{r=1}^m \Delta \tau_{ij}^r, \quad (3)$$

where  $(1 - \omega)$  is a pheromone declining rate and  $\Delta \tau_{ij}^r$  is the pheromone quantity present in the route  $(i,j)$ , most recently updated by the  $m$ th ant. The pheromone concentration is modeled with the travel time of the vehicle. Therefore, the pheromone ceasing is due to energy drain of the vehicle or higher charging time, unplanned tour path, and incomplete traversal. If either of the conditions is achieved, then the pheromone ceases with the varying time interval. Unlike in traditional ACO process, the low pheromone ant pursues a higher pheromone ant if there is a common intersecting DP for two or more ants. A DP that is reached by two or more ants through different neighboring DPs increases the chances of intersection. For a pheromone-based ant route discovery, there is an analysis briefed as below. Figure 3 illustrates the case of common intersecting DP by two ants:  $a_1$  and  $a_2$ .

### 3.5.1 | Pheromone analysis

If the intersection of the ants at a common DP is true and either of the ant holds a higher pheromone in the next regular link.

### 3.5.2 | Solution

Let  $a_1$  and  $a_2$  be the ants with different pheromone concentration. If  $t_{tr}(a_1) < t_{tr}(a_2)$  and  $\tau_{ij}(a_1) > \tau_{ij}(a_2)$ , then compute the additional time request by  $a_1$  to visit the DP of  $a_2$  using Equation (4):

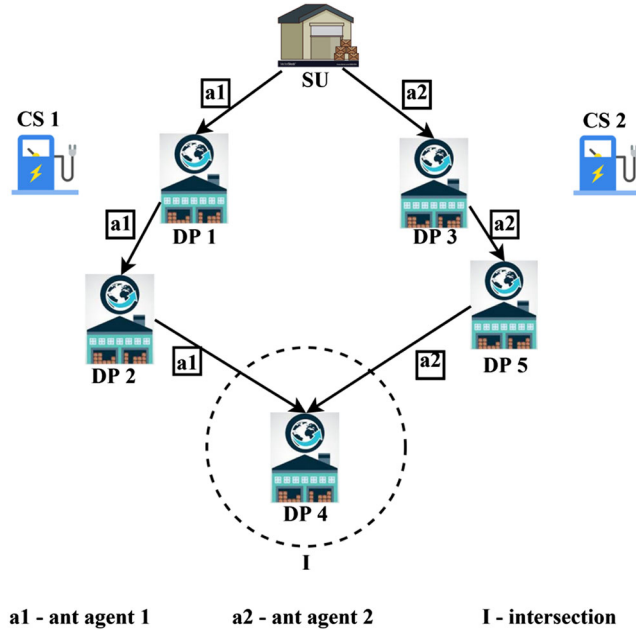


**FIGURE 3** Intersecting delivery point (DP) illustration

$$t_{tr}(a_1) = t_{tr}(a_1) + t_{tr}(dp_{a1}, dp_{a2}), \quad (4)$$

where  $dp_{a1}$  and  $dp_{a2}$  are the DPs assigned for ants  $a_1$  and  $a_2$ , respectively.

If  $\sum \frac{t_{tr}(a_1)}{dp_{a1}} < t_c$  and  $t_c < t$ , then the route plan of  $a_1$  is modified to visit  $dp(a_2)$ . Similarly,  $a_2$  skips the intersecting DP and changes its route plane to visit the next DP.

Changing the route plane of  $a_2$  (low pheromone) does not cause an adverse effect in time; ie, the delay in  $a_2$  completion is reduced compared with the estimated initial route plan.

Contrarily, delay of  $a_1$  increases because of the inclusion of additional DP. In this condition, a new ant is generated to share the route plan of  $a_1$ . That is, the ant with the least pheromone (0 as it has not visiting any DP) will pursue  $a_1$ . The route plan of  $a_1$  is revised to cooperate with the new ant agent such that the pheromone of the new ant is computed after “x” distance from its initial position. The distance “x” represents the displacement of the  $a_1$ -included DP from the source point. Now,

$$\Delta t_{tr}(a_1) = t_{tr}(dp_1) + t_{tr}(dp_2) + \dots + t_{tr}(dp_k), \quad k < dp(a_1), \quad \text{then } t_{tr}^*(a_1) < t_{tr}(a_1), \quad (5)$$

where  $t_{tr}^*(a_1)$  is the current travel time observed by  $a_1$ .

Equation (5) determines the total travel time of the agent 1, in which the EV instigates its route plan if  $\tau_{ij}(a_1) > \tau_{ij}(a_2)$ . The above probability is estimated for a vehicle starting from SU and visiting all DPs with the need of demand link. Let  $\gamma_{u,v}$  denote the probability of a vehicle  $v$  being charged at CS “u,” then

$$\Delta t_{tr}(a_1) = \Delta t_{tr}(a_1) + (t_c * \gamma_{u,v} * \rho_{1u}^{dist}). \quad (6)$$

For a graph  $G = (v, rl)$ ,  $\Delta t_{tr}$  is estimated using Equation (5), and for a graph  $G = (v, dl \cup rl)$ ,  $\Delta t_{tr}(a_1)$  is estimated as in Equation (6).

The aforementioned analysis provides solution for the travel time observed under different pheromone concentrations. The following section describes the intersection analysis of two or more ants with the precise travel time estimation. The effects of pheromone concentration and intersection at the common point are discussed in the previous and following analysis, respectively.



### 3.6 | Intersection analysis

The progress in optimality is defined by identifying delay-less route plan. The delay-less route plan is computed by identifying next DP from the current position, before leaving the current DP.

The region of intersection of two/more ant agents needs to be left out for delay-less route plan. The left-out DP is accessed by the new ant agent. For the next detouring process, either of the ants must mutually be exclusive of their visiting DPs. The ant that is approaching from a farthest distance to the IA detours its route.

The intersecting area (IA) in Figure 4 is the summation of the range both ants  $a_1$  and  $a_2$ , ie,

$$IA = [A(a_1) + A(a_2)], \quad (7)$$

where  $A(a_1)$  and  $A(a_2)$  are the coverage region observed at a segment S. Let  $rd_1$  and  $rd_2$  be the radius of  $a_1$  and  $a_2$ , respectively; then,

$$A(a_1) = rd_1^2 * \theta_1 - \frac{rd_1^2 * \sin 2\theta_1}{2} \text{ and } A(a_2) = rd_2^2 * \theta_2 - \frac{rd_2^2 * \sin 2\theta_2}{2}. \quad (8)$$

Substituting (8) in Equation (7),

$$IA = rd_1^2 * \theta_1 - \frac{rd_1^2 * \sin 2\theta_1}{2} + rd_2^2 * \theta_2 - \frac{rd_2^2 * \sin 2\theta_2}{2}. \quad (9)$$

If both the ant agents are toward the same DP, then with respect to their bisector angle of deviation,  $\theta_1 = \theta_2 = 45^\circ$ .

$$\begin{aligned} IA &= rd_1^2 * 45 - \frac{rd_1^2 * \sin 90^\circ}{2} + rd_2^2 * 45 - \frac{rd_2^2 * \sin 90^\circ}{2} \\ &= rd_1^2 * 45 - \frac{rd_1^2}{2} + rd_2^2 * 45 - \frac{rd_2^2}{2} \\ &= rd_1^2 * \frac{\pi}{4} - \frac{rd_1^2}{2} + rd_2^2 * \frac{\pi}{4} - \frac{rd_2^2}{2} \\ IA &= (rd_1^2 + rd_2^2) * \frac{\pi}{4} - \frac{1}{2}(rd_1^2 + rd_2^2) \end{aligned} \quad (10)$$

The angle of deviation changes with the velocity and position of the vehicle, where in a constant deviation as defined above is not possible. Equations (9) and (10) hold for any angle of deviation, depending upon which the intersecting area of the vehicles changes. The intersecting area of the vehicles is located within their coverage; the range varies with the angle of deviation.

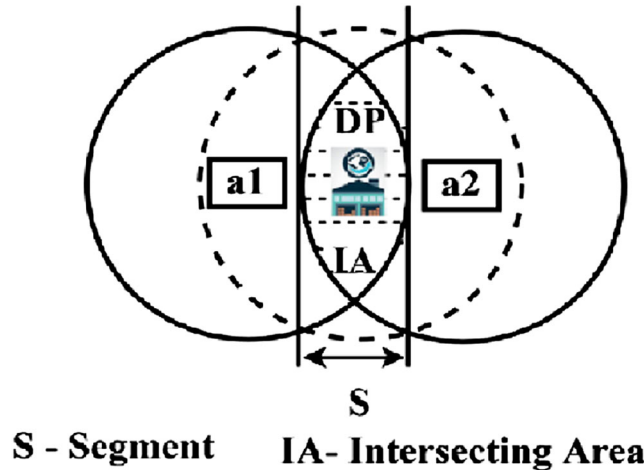


**FIGURE 4** Intersecting area illustration

Thus, the intersection region of both the agents is estimated. Now, the distance between the agents and IA is computed to identify the nearest approaching agent. The ant agent with lesser distance visits the DP in IA. Higher distance ant agent will detour its path to visit the next DP; the probability of a longest distance ant to visit the intersection DP is 0 (i.e.)  $\rho_{ij}^{\text{dist(IA)}}(t) = 0$ . In a detouring approach, a few other DP is either included/excluded from the initial route plan because of which  $t_{tr}$  of an agent varies. The solution is defined as a probability density function as  $[\varphi(t_{tr})]$ .

$$\varphi(t_{tr}) = \sigma * \text{dist}(i, j) * c_i^{\sigma-1}, \quad (11)$$

where  $\sigma$  is the average number of ant visits and  $c_i^{\sigma-1}$  is a complementary function of  $t$ .

Now,  $\varphi(t_{tr}) = \sigma * \int_0^{ev_v^t} ev_v^t dv^t \left[ 1 - \int_{t=0}^{\infty} ev_v^t dt \right]^{\sigma-1}$ . The average time of travel is computed using Equation (12):

$$\text{avg}(t_{tr}) = \int_0^{\theta} t_{tr} \cdot \varphi(t_{tr}) \cdot dt_{tr} \text{avg}(t_{tr}) = \int_0^{\theta} t_{tr} * \sigma * \text{dist}(i, j) * \left[ 1 - \int_{t=0}^{\infty} ev_v^t dt \right]^{\sigma-1}. \quad (12)$$

As per the objective, for an EV that excludes a DP in IA, then its  $t_{tr}$  is less than the initial planned time, ie,  $t_{tr} < t_c < t$ . For an EV that adds up additional DP in its route tour plan, if  $t_{tr}^* + t_c > t$ , then a new ant agent is assigned to visit the DP from which the new ants time of travel is estimated. If an ant is subject to visit additional DP other than its initial list, then the ant is overloaded. This increases the travel time and charging time of the vehicle exceeding its initial operation time. In such a scenario, the average time of travel of all the ant agents will remain within the expected  $t$ . The paths formulated by the ant agents will be fed to the EV to instigate the tour for DPs.

### 3.7 | Range-sustained traversing

Range-sustained traversing is designed to prolong the driving range of the EV. This covers maximum DP before requiring demand links. In this traversing node, the vehicle is restricted to communicate to its like neighbors other than DPs. EV routes to the CS from the most recently visited DP. The routes are identified from the solutions of conditional route discovery after estimating the  $t_{tr}$ . The time travel of the identified routes is considered with the intersection analysis to identify the correctness of the routes with respect to delay. Considering the power of the EV along with delay needs to be addressed in a synchronized manner. A fitness function that balances both energy and delay to achieve optimal solution is formulated. The fitness function inputs the possible level of energy and characteristics and frames rules to conclude with the better solution. The rules define the process of path selection and determine the travel time. The optimality in path selection and visiting is tuned with the pheromone and intersection analysis. The range of the intersecting area and the visiting time is dependent on the energy of the vehicles. The battery power of the vehicle is utilized with the discussed considerations. The conclusion results in discovering energy efficient rates that retains the driving range of the vehicles.

The battery power utilization  $p_b$  of an EV is estimated using Equation (13):

$$p_b = \frac{ev_u^t}{\mu} \left( Wg\delta_{rr} \cos\theta + Wg\sin\theta + \frac{1}{2}\delta_a \omega_d v_f (ev_v^t)^2 + W\Delta\omega \frac{dev_v^t}{dt} \right), \quad (13)$$

where

$\mu$  = parameter for efficiency,

$W$  = weight of the EV,

$g$  = gravitational constant,

$\delta_{rr}$  = coefficient for rolling resistance,

$b_a$  = density of air,



$\omega_d$  = coefficient for aerodynamic drag,

$v_f$  = frontal area of the vehicle,

$\Delta\omega$  = weight factor of  $w$ , and

$\frac{dev_u^t}{dt}$  = acceleration.

Similarly, the battery power spent at the time of breaking ( $p_{bb}$ ) is computed using Equation (14):

$$p_{bb} = \frac{yev_u^t}{\mu} \left( Wg\delta_{rr} \cos\theta + Wg\sin\theta + \frac{1}{2}\delta_a \omega_d v_f (ev_v^t)^2 + W\Delta\omega \frac{dev_v^t}{dt} \right). \quad (14)$$

The total power consumed ( $tp_b$ ) is now estimated as

$$tp_b = \int_{travel\ t} P_b + \int_{breaking\ t} P_{bb}. \quad (15)$$

Consider the graph model as in Figure 5A.

Considering  $p_{bb}$  and  $t_{tr}$  as the input for framing rules, the fitness function is defined. The fitness function  $\Omega(r)$  is evaluated as a disjoint solution considering both travel time and battery power, the preference being provided for battery power. Equation (16) defines the fitness of a route  $r$  as

$$\Omega(r) = \varphi_1 * \Delta t_{tr} + \varphi_2 * tp_b, \quad (16)$$

where  $\varphi_1$  and  $\varphi_2$  are the balancing coefficients and  $\varphi_1 + \varphi_2 = 1$ . For  $(p_r - tp_b) < p_{min}$ ,  $\varphi_2 > \varphi_1$ . The output of (16) categorizes the solution for different range of inputs. Obviously, the route to DP or CS with higher  $\Omega(r)$  is selected for next visit. If  $r = \{r_1, r_2, \dots, r_n\}$  represents a set of routes, then  $\max\{\Omega(r_1), \Omega(r_2), \dots, \Omega(r_n)\}$  is the optimal solution. The second largest fitness value will be the near to optimal solution and so on. If  $(p_r - tp_b) > p_{min}$  or  $tp_b > p_{min}$ , then the solution is terminated to initiate a new route plan. Table 1 illustrates the characteristics of the considered inputs.

The first two solutions are considered to be optimal with the existing and new ant agents. The routes established with the plans of the first two solutions will be energy efficient to improve the driving range of the EV. For the figure above, the conventional tour plan as per solution 1 is

$$SU - dp1 - dp2 - dp4 - dp5 || dp5 - cs2 - dp3 - SU.$$

In this tour plan, the EV establishes demand link to recharge its battery power. The number of vehicles present in the nearest CS is unknown. As the CSs are placed in a dispersed manner, CS discovery needs to be related with distance. In this condition, the charging time of the vehicle is considered such that  $t_{tr}^* + t_c < t$  is maintained. The minimum power required to visit the CS is retained by the vehicle to pursue further routing. The minimum power  $p_{min}$  required to transit the EV to the CS from the current position is computed using Equation (17):

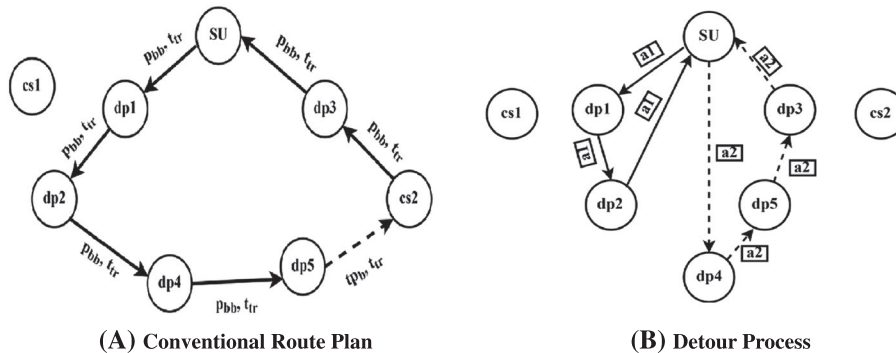


**FIGURE 5** A, Conventional route plan. B, Detour process

**TABLE 1** Input characteristics and solution

$p_{bb}$	$t_{tr}$	Solution	Route Tour
Low	Low	Move to next DP	Add DP to the EV route
Low	High	New ant agent	Exclude DP and detour
High	Low	Terminate	New route plan
High	High	Terminate	New route plan

Abbreviations: DP, delivery point; EV, electric vehicle.

$$p_{\min} = \frac{p_r - tp_b}{\sigma - 1}, \text{dist}(dp, cs) < (ev_v^t * t_{tr}^*), \quad (17)$$

where  $p_r$  is the power of the EV when initiating route traversal from SU. The number of visits by the ant agents represents the DP or DP + CS visited so far in the traversal.

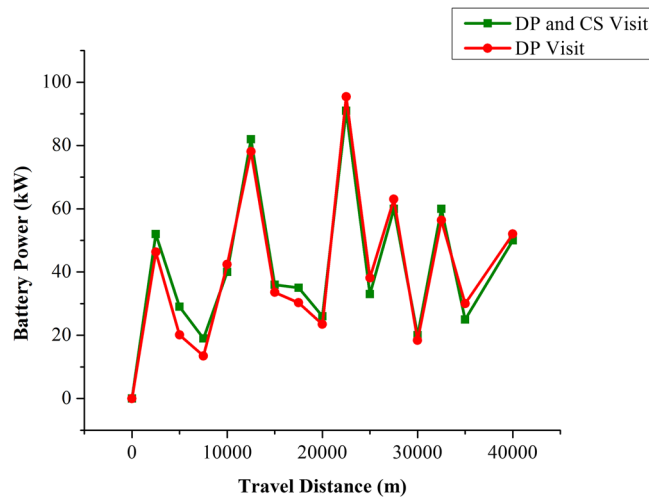
As per the solution 2, the tour plan is represented as follows (refer Figure 5B):

$$SU - dp1 - dp2 - SU,$$

and

$$\left. \begin{array}{l} SU - dp4 - dp5 - dp3 - SU \\ \text{or} \\ SU - dp3 - dp5 - dp4 - SU \end{array} \right\} \in \text{new agent}.$$

Here, dp4 is excluded by a1 as a2 intersects at the same position, and hence, the new agent (a2) traverses the route independently. The above routes are identified by satisfying energy utilization of the vehicle with lesser travel time; the travel time falls in the category of the either of the pheromone concentration observed in the ants. Here, the first solution satisfies  $p_{\min}$ , and the second set of solution is instigated by the new agents for which intersection analysis and time travel are estimated. If the new agent satisfies the pheromone concentration level, then the new path is switched for traversing.

**FIGURE 6** Battery power analysis

## 4 | EVALUATION

### 4.1 | Evaluation setup

The proposed FACO for EVs is evaluated through an experimental setup modeled using SUMO network simulator. The battery capacity of the vehicle is 24 kWh. The vehicle holds a coverage range of 150 to 200 mts, with  $v_f = 1.50$  m. The power utilization of an EV is estimated for 400-kg payload with 10% of loss consideration. The scenario is modeled with four CSs and 100 EVs.

## 5 | DISCUSSION

### 5.1 | Battery power analysis

Figure 6 analyzes the battery power expenditure for DP and CS visits in a cumulative and independent manner. With the increasing travel distance, the power expenditure of the vehicles increases. The cumulative power for a route plan is computed for the different agents employed. The visits are planned in a time-dependent routing model to minimize unnecessary or idle power depletion. DP and CS visit in a long route plan is subjected to vary with range of the vehicle and the number of other agents instigated. The distance factor plays a crucial role in determining the battery exhaustion rate of the vehicle. The minimum power requirement to reach the CS is also considered such that the total power consumption in a DP and CS visit is less at some points. Power requirement in individual visits between successive DPs or while establishing a demand link is considered. The average energy of all the vehicles that participate either in a regular tour plan or detour is computed. The independent power values of a vehicle are subjected to change with respect to its position and displacement from the next DP or CS. However,  $p_{\min}$  is the required power for routing an EV to the CS. The mean power in DP and CS visit and DP visit with its difference is tabulated in Table 2.

### 5.2 | Peak load analysis

The average peak load observed at the CSs is illustrated in Figure 7. Because of inexpensive cost of placement, a few CSs are deployed in a distributed manner across the city environment. Lesser is the number of CS; vehicle crowd feed at a

**TABLE 2** Power variation analysis

Mean DP and CS Visit Power (kWh)	Mean DP Visit Power (kWh)	Difference (kWh)
12.653 85	13.845 14	−1.191 29
20.896 55	29.588 56	−8.692 01
30.368 42	42.659 99	−12.2916
13.95	13.241 15	0.708 849
6.3170 73	6.641 659	−0.324 59
14.888 89	16.091 37	−1.202 48
17.142 86	19.969 31	−2.826 45
25.346 15	28.537 28	−3.191 13
7.945 055	7.718 029	0.227 026
21.666 67	19.096 15	2.570 518
12.783 33	12.392 54	0.390 794
39.25	43.409 24	−4.159 24
13.983 33	15.237 53	−1.2542
34.2	29.166 67	5.033 333

*Note.* The negative values in the difference field indicate the saved power as the EV has not visited the DP. Either the DP has existed in intersection, or the EVs have detoured its visit with the next DP in this case.

Abbreviations: CS, charging station; DP, delivery point.

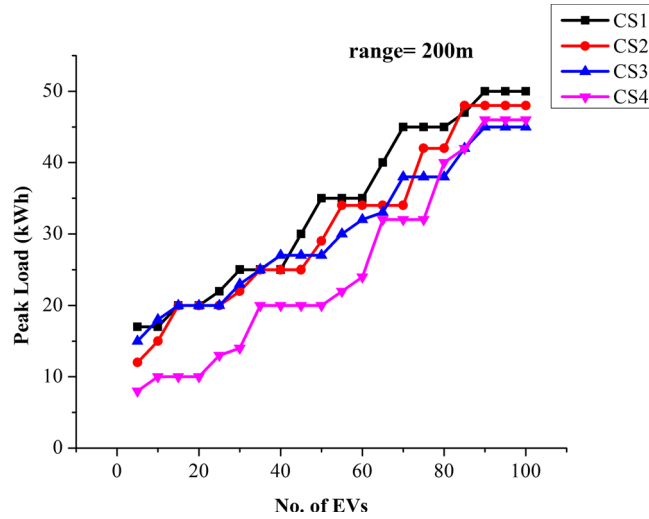


FIGURE 7 Peak load observations

particular CS is high. Peak load observed at each of the CS increases with  $t_c$ . The wait time of the series of vehicles requesting demand links will increase the charging time of the EV. To retain the cost effectiveness and also to provide timely charging, the CS needs to be modeled with synchronized opportunistic admission schemes.

### 5.3 | Comparative analysis

The proposed FACO is compared with EV navigation-based on crowd sensing (EVNCS)<sup>15</sup> and mobile energy disseminators route optimization<sup>28</sup> (MED-RO) for charge level,<sup>23</sup> driving distance, energy depletion, waiting time, and average visits.

### 5.4 | Analysis of charge level

Charge level is estimated as the ratio of difference between remaining and initial energy of the vehicle observed between two charging intervals. It is mathematically expressed as

$$\text{charge level (\%)} = \frac{\text{Total Battery Power} - p_b}{\text{Total Battery Power}} \times 100.$$

An EV traveling longer distance needs battery recharge to further pursue the travel. The available charge level for the EV over the increasing travel distance is illustrated in Figure 8. Distance, power loss, and payload of the vehicle decide the charge level of the battery. The charge level of EV battery is estimated before it requests demand link. For the observed charge level, recharging the vehicle battery depends on the number of intersections and DPs. If  $(p_r - p_b) < p_{\min}$ , then the vehicle requests demand link to retain its charge level. In the other existing approaches, the diminishing vehicle efficiency is accounted for recharge wherein the available charge level is comparatively less.

### 5.5 | Analysis of driving distance

The driving range of the vehicles with the aid of CS for the existing approaches and the proposed FACO are compared in Figure 9. The optimal route plan based on time and delay with the consideration of  $t_c$  is evaluated in the proposed FACO. The availability of CS is considered in the route plan of the EV, and the more delay-less route is selected for visiting the DP. This ensures that the demand link is also discovered with a lesser time, projecting the priority of the vehicle at the charge station. With the aid of charging, the actual  $t_c$  within  $t$  is less, recommending prolonged distance coverage by the EV. Unlike the other methods,  $p_{\min}$  determines the recharging state of the EV, sustaining DP exclusion from the route plan.

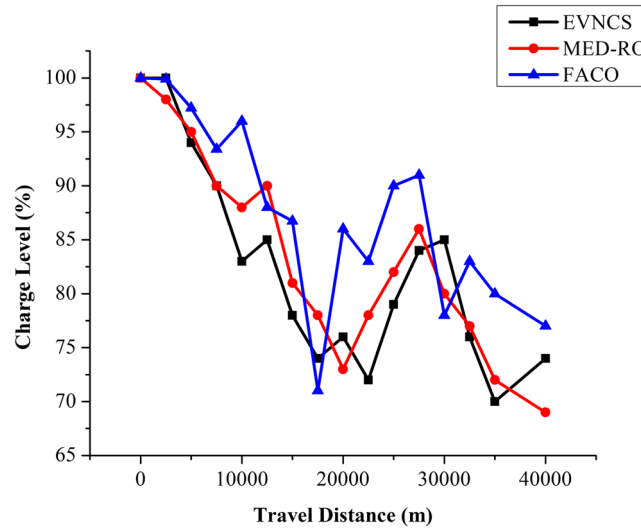


**FIGURE 8** Charge level analysis

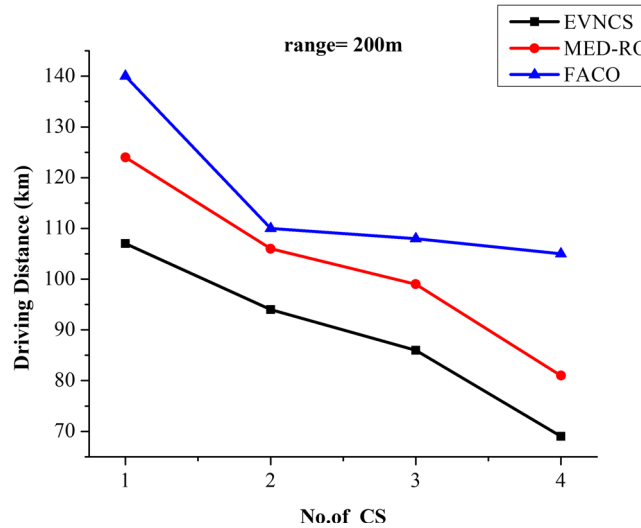


**FIGURE 9** Driving distance analysis

## 5.6 | Depletion power analysis

The unnecessary power being depleted in a complete route plan is compared between the existing and the proposed FACO in Figure 10. EV's efficiency ceases with travel time and distance as the battery requires recharging. Power depletion because of unplanned route plan is confined through conditional route discovery process where  $t_c \leq t$  is retained over every route of  $G$ . The vehicle is directed to identify the nearest CS path by determining delay-less routes by examining the pheromone of next DP or CS availability. The vehicle controls unnecessary detours when  $p_{\min}$  is achieved. Therefore, battery expenditure is controlled in both routing and traversing, minimizing depletion power.

## 5.7 | Waiting time analysis

EV's experience waiting time depending on the number of former EVs queued in the CS. If the count of queued EVs is high, then wait time of the next EV increases. Through a conditional route discovery, travel time is confined that it does not exceed  $t$ .  $\Delta t_{tr}$  for the overall visit endorses the waiting time that satisfies the objective function. With the mutual exclusion of intersection region, the vehicles alter their initial route plan; the new agents are intended to retain

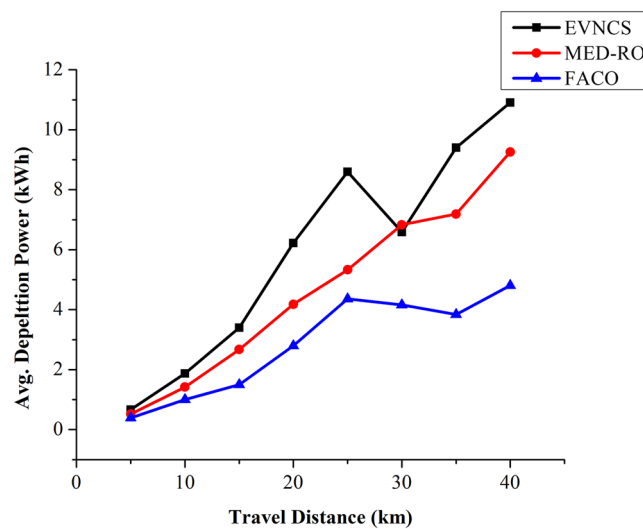


FIGURE 10 Average depletion power comparison

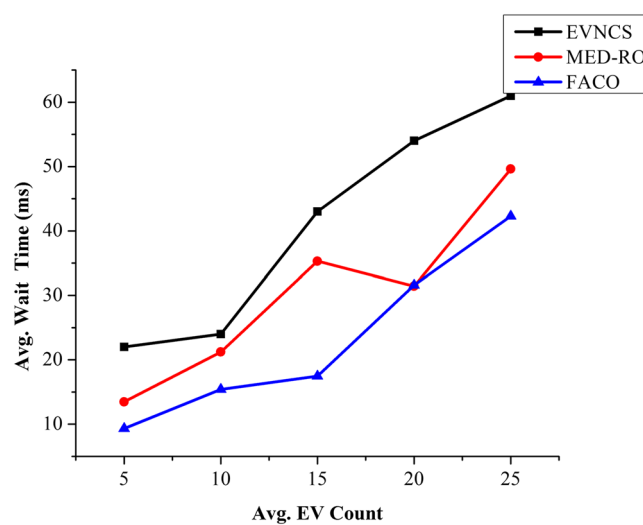


FIGURE 11 Wait time comparison

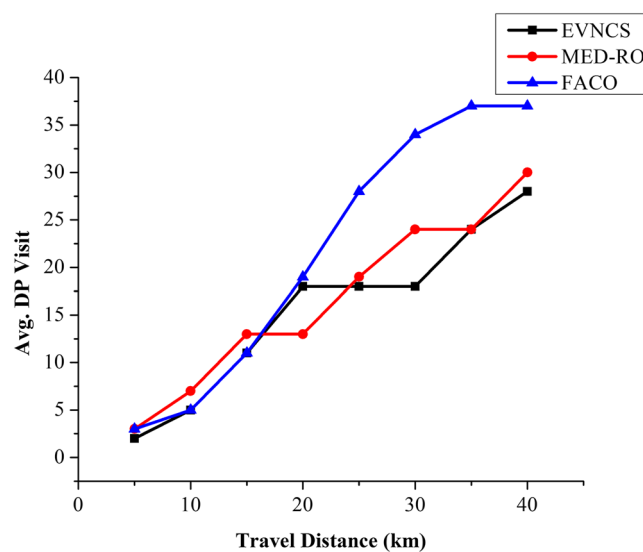


FIGURE 12 Average delivery point (DP) visit comparison



delay-less traversing between DPs and DP to CS. Therefore, the average wait time of a  $p_{\min}$  vehicle is less in FACO compared with the other approaches (Figure 11).

## 5.8 | Average visit analysis

The average number of DP visits of the proposed FACO is compared with the existing EVNCS and MED-RO in Figure 12. The initial route plan of the EVs is altered depending on the power and delay factors. If delay is found to be increasing, then a new agent is generated to mitigate additional visiting time. The intersecting DPs are mutually visited by either of the EVs, minimizing the visiting time. The minimized visiting time is spent for visiting a new DP with the detour or additional route plans. The stagnancy in visiting DP occurs when  $(p_r - tp_b) < p_{\min}$  is true. The vehicle requires  $t_c$  to recharge its battery and proceeds further traversing.

## 6 | CONCLUSION

This manuscript introduces a fitness-based ant colony optimization for improving route discovery and traversing process to improve the driving range of EVs. The proposed method operates in two phases to discover conditional routes and ensure sustained traversing. Conditional route discovery minimizes travel time of the vehicles through optimal graph route visiting plan. Sustained route traversing addresses the energy demands of EVs to conserve battery power and ensure prolonged driving range. The assimilated phases work in a cooperative manner to minimize routing complexities in EV technology. FACO is found to improve routing performance by retaining 7.15% of charge level, increasing the driving distance by 28.58%, minimizing depletion power by 51.99%, and waiting time by 30.67% and increases the ratio of DP visits by 21.62% compared with the existing methods, respectively. The future work is planned to integrate the concept of on-demand in-vehicle charging harmonizing with the mobility and direction of movement to further reduce CS peak load.

## ORCID

Gunasekaran Manogaran  <https://orcid.org/0000-0003-4083-6163>

## REFERENCES

1. Hackmann H, Moser SC, Clair ALS. The social heart of global environmental change. *Nat Clim Change*. 2014;4(8):653-655.
2. Zanella A, Bui N, Castellani A, Vangelista L, Zorzi M. Internet of Things for smart cities. *IEEE Internet Things J*. 2014;1(1):22-32.
3. Boriboonsomsin K, Barth MJ, Zhu W, Vu A. Eco-routing navigation system based on multisource historical and real-time traffic information. *IEEE Trans Intell Transp Syst*. 2012;13(4):1694-1704.
4. Dey KC, Yan L, Wang X, et al. A review of communication, driver characteristics, and controls aspects of cooperative adaptive cruise control (CACC). *IEEE Trans Intell Transp Syst*. 2016;17(2):491-509.
5. Shao S, Guan W, Ran B, He Z, Bi J. Electric vehicle routing problem with charging time and variable travel time. *Math Probl Eng*. 2017;2017:1-13.
6. Papavasiliou A, Oren SS, Oneill RP. Reserve requirements for wind power integration: a scenario-based stochastic programming framework. *IEEE Trans Power Syst*. 2011;26(4):2197-2206.
7. Yang H, Pan H, Luo F, et al. Operational planning of electric vehicles for balancing wind power and load fluctuations in a microgrid. *IEEE Trans Sustainable Energy*. 2017;8(2):592-604.
8. Saber AY, Venayagamoorthy GK. Plug-in vehicles and renewable energy sources for cost and emission reductions. *IEEE Trans Ind Electron*. 2011;58(4):1229-1238.
9. Shao S, Guan W, Bi J. Electric vehicle-routing problem with charging demands and energy consumption. *IET Intell Transp Syst*. 2018;12(3):202-212.
10. Amjad S, Neelakrishnan S, Rudramoorthy R. Review of design considerations and technological challenges for successful development and deployment of plug-in hybrid electric vehicles. *Renew Sustain Energy Rev*. 2010;14(3):1104-1110.
11. Chen X, Sun H, Tobe Y, Zhou Z, Sun X. Coverless information hiding method based on the Chinese mathematical expression, In: Cloud Computing and Security Lecture Notes in Computer Science, Springer, Cham, China 2015:133-143.
12. Bulut E, Kisacikoglu MC. Mitigating range anxiety via vehicle-to-vehicle social charging system, In: 2017 IEEE 85th Vehicular Technology Conference (VTC Spring); IEEE, Australia 2017.

13. Bozorgi AM, Farasat M, Mahmoud A. A time and energy efficient routing algorithm for electric vehicles based on historical driving data. *IEEE Trans Intell Vehicles*. 2017;2(4):308-320.
14. Xue Y, Jiang J, Zhao B, Ma T. A self-adaptive artificial bee colony algorithm based on global best for global optimization. *Soft Comput*. 2017;22(9):2935-2952.
15. Yang H, Deng Y, Qiu J, Li M, Lai M, Dong ZY. Electric vehicle route selection and charging navigation strategy based on crowd sensing. *IEEE Trans Ind Inf*. 2017;13(5):2214-2226.
16. Al-Mayouf YRB, Abdullah NF, Mahdi OA, et al. Real-time intersection-based segment aware routing algorithm for urban vehicular networks. *IEEE Trans Intell Transp Syst*. 2018;19(7):2125-2141.
17. Alsharif N, Shen X. \$i\$CAR-II: infrastructure-based connectivity aware routing in vehicular networks. *IEEE Trans Veh Technol*. 2017;66(5):4231-4244.
18. Lin D, Kang J, Squicciarini A, Wu Y, Gurung S, Tonguz O. MoZo: a moving zone based routing protocol using pure V2V communication in VANETs. *IEEE Trans Mob Comput*. 2017;16(5):1357-1370.
19. Song J, Zhang J, Fan X. Routing protocol for battery management system of electric vehicles based on ad-hoc network. *IET Netw*. 2018;7(5):283-286.
20. Yu JJQ, Lam AYS. Autonomous vehicle logistic system: joint routing and charging strategy. *IEEE Trans Intell Trans Syst*. 2018;19(7):2175-2187.
21. Li C, Ding T, Liu X, Huang C. An electric vehicle routing optimization model with hybrid plug-in and wireless charging systems. *IEEE Access*. 2018;6:27569-27578.
22. Chen T, Zhang B, Pourbabak H, Kavousi-Fard A, Su W. Optimal routing and charging of an electric vehicle fleet for high-efficiency dynamic transit systems. *IEEE Trans Smart Grid*. 2018;9(4):3563-3572.
23. Kosmanos D, Maglaras LA, Mavrovouniotis M, et al. Route optimization of electric vehicles based on dynamic wireless charging. *IEEE Access*. 2018;6:42551-42565.
24. Schuster A, Bessler S, Grønbaek J. Multimodal routing and energy scheduling for optimized charging of electric vehicles. *e & i Elektrotechnik und Informationstechnik*. 2012;129(3):141-149.
25. Boysen N, Briskorn D, Emde S. Scheduling electric vehicles and locating charging stations on a path. *J Sched*. 2017;21(1):111-126.
26. Hassan AN, Abdullah AH, Kaiwartya O, Cao Y, Sheet DK. Multi-metric geographic routing for vehicular ad hoc networks. *Wirel Netw*. 2017;24(7):2763-2779.
27. Schneider M, Stenger A, Hof J. An adaptive VNS algorithm for vehicle routing problems with intermediate stops. *OR Spectr*. 2014;37(2):353-387.
28. MuhammedShafi. P, Selvakumar S\*, Mohamed Shakeel. P, "An efficient optimal fuzzy C means (OFCM) algorithm with particle swarm optimization (PSO) to analyze and predict crime data", *J Adv Res Dyn Control Syst* 2018;10(06):699-707.

**How to cite this article:** Manogaran G, Shakeel PM, Priyan R V, Chilamkurti N, Srivastava A. Ant colony optimization-induced route optimization for enhancing driving range of electric vehicles. *Int J Commun Syst*. 2019;e3964. <https://doi.org/10.1002/dac.3964>